

# Integration of Finite-Element Analysis and Numerical Optimization Techniques for RAM Transport Package Design\*

*D.C. Harding, M.S. Eldred, W.R. Witkowski  
Sandia National Laboratories*

## INTRODUCTION

Type B radioactive material transport packages must meet strict Nuclear Regulatory Commission (NRC) regulations specified in 10 CFR 71. Type B containers include impact limiters, radiation or thermal shielding layers, and one or more containment vessels. In the past, each component was typically designed separately based on its driving constraint and the expertise of the designer. The components were subsequently assembled and the design modified iteratively until all of the design criteria were met. This approach neglects the fact that components may serve secondary purposes as well as primary ones. For example, an impact limiter's primary purpose is to act as an energy absorber and protect the contents of the package, but can also act as a heat dissipater or insulator. Designing the component to maximize its performance with respect to both objectives can be accomplished using numerical optimization techniques.

A simple Type B package overpack design was selected (see Figure 1) to demonstrate the effectiveness of numerical optimization's use in RAM package design. This small Department of Transportation 6M-like packaging developed at Sandia National Laboratories (Pierce et al. 1992) was designed to meet present and future regulatory requirements, including a proposed 10 CFR 71 change adding dynamic crush resistance (500 kg steel plate dropped 9 m onto the package). This package design uses nested stainless steel cylindrical containment vessels (double containment for plutonium powder cans) with threaded closures and elastomeric seals. The overpack consists of layers of aluminum wire mesh, which provide excellent impact energy absorption through individual wire deformation and thermal insulation via numerous trapped air pockets between wires. Layered ceramic cloth material provides additional thermal insulation. A simplified geometry was selected to represent the wire mesh and ceramic cloth overpack. The nested containment vessel design is assumed fixed. The model consists of one structural impact limiter material layer (wire mesh) sandwiched between two thermal

\* This work was supported by the U. S. Department of Energy under contract number DE-AC04-94AL85000.

insulation material layers (ceramic cloth). The geometric model is defined by six design variables which represent the radial and longitudinal material thickness for each layer.

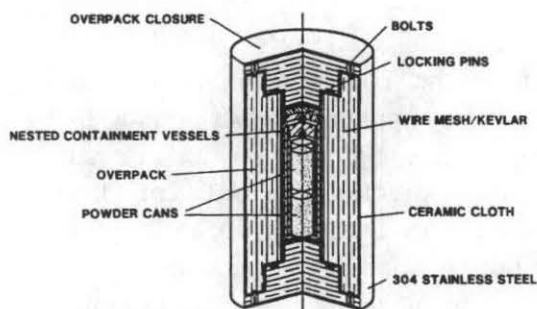


**Figure 1. Type B Ram Transport Container With Wire Mesh Composite Overpack**

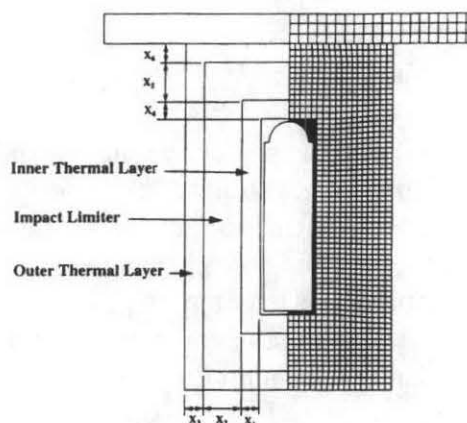


**Figure 2. Six Overpack Layer Thicknesses Or Design Variables**

The six design variables are shown in Figure 2. The two primary accident conditions modeled include a 500 kg plate dropped from 9 m onto the package and a 30-minute 800° C fire. The respective design constraints associated with each of these accident conditions are (1) deformation in the containment vessel seal region remains small enough to satisfy NRC regulations for end-on and side-on configurations, and (2) the elastomeric seal region stays below its operational temperature limit to ensure seal integrity in the fire environment.

The goal of the design exercise is to minimize the overpack weight (or mass) while satisfying the thermal and structural design constraints. Separate optimization problems for thermal and end-on impact conditions were used initially to evaluate code integration, performance, and design problem nonlinearities. Finite element analyses were used to predict dynamic structural and transient thermal behavior of the container and evaluate the constraints. Simplified finite element models of the package were developed to reduce the computational cost of successively running numerous analyses within the optimization framework. Substantial effort has been put forth to develop these simplified models, balancing accuracy with minimal computational run time.

## CODE INTEGRATION AND OPTIMIZATION MODEL DEVELOPMENT

The iterative design, analysis, and redesign process must be automated for the optimization design tool to be efficient and viable. This automation requires the nontrivial integration of numerical simulation and optimization algorithms, including the manipulation of data between the two routines. The FASTQ (Blacker 1988) automatic mesh generation algorithm was used to generate finite element analysis (FEA) input files from the geometric sizing (design) variables. The explicit structural FEA code PRONTO (Taylor and Flanagan 1987) and the transient thermal FEA code COYOTE (Gartling 1993) were used to evaluate accident condition design constraints using the DOT (Vanderplaats 1994) optimization software within the DAKOTA (Eldred et al. 1995) optimization toolkit. The modified method of feasible directions for constrained numerical optimization was used to minimize the overpack weight (called the objective function) subject to the constraints through

systematic variation of the six design variables. The optimization problem can be stated mathematically as,

$$\text{minimize } F(x) \quad (1)$$

$$\text{subject to } g_i(x) \leq 0 \quad i = 1, k \quad (2)$$

where  $F(x)$  is the objective function and  $x$  is a vector of the six design variables. Equation 2 is a series of constraints on the design variables, such as upper and lower bounds and required resistance to structural and thermal accident environments. Evaluation of equation 2 requires meshing the current geometry and performing structural and/or thermal finite element analysis to determine the peak stress or temperature in the seal area and compare it with its maximum allowable value. Thus, as the optimization routine searches numerically for a minimum weight geometry, many separate analyses are performed.

### Dynamic Crush Model

One of the accident environments involves dropping a 500 kg rigid steel plate on the package in a worst-case orientation. Detailed end-on and side-on finite element analyses were performed to calibrate a simplified and faster, yet accurate FEA model to perform overpack optimization based upon structural design constraints, and the results have been presented previously (Harding and Eldred 1995). Only the thermal and combined (structural and thermal) optimization results are presented in this paper.

### Thermal Model

The axisymmetric 2-D model developed for transient thermal analysis was visually similar to that shown in Figure 2, except that only one-fourth of the mesh was generated due to symmetries. Material properties for ceramic cloth insulation (Siltemp 84CH) were provided by the manufacturer, and temperature-dependent properties for wire mesh were measured experimentally (Wix and Pierce 1995). The density of wire mesh wrapped tightly around the containment vessels is approximately  $450 \text{ kg/m}^3$ , while that of the ceramic cloth is approximately  $800 \text{ kg/m}^3$ . Temperature-dependent thermal conductivity and specific heat for aluminum wire mesh and ceramic cloth insulation are compared in Figures 3 and 4. Boundary conditions include an internal heat generation of 20 W (from decay of plutonium oxide) applied as a constant effective heat flux to the inner overpack surface. A transient heat flux associated with radiation and still air convection to a surrounding fire temperature of  $800^\circ \text{C}$  was applied to the overpack's external surface (emissivity=0.9) for 30 minutes, simulating the fuel fire accident condition. Seal area temperatures were tracked beyond the point at which seal temperatures began to decline (3.5 hours after application of the external heat load), and the peak temperature was used for constraint evaluation.

The highest allowable operating temperature for the elastomeric (Viton) O-ring seals is approximately  $232^\circ \text{C}$ ; thus the constraint value is defined by:

$$g_2 = T_{\text{inner wall}} - 232 \leq 0 \quad (3)$$

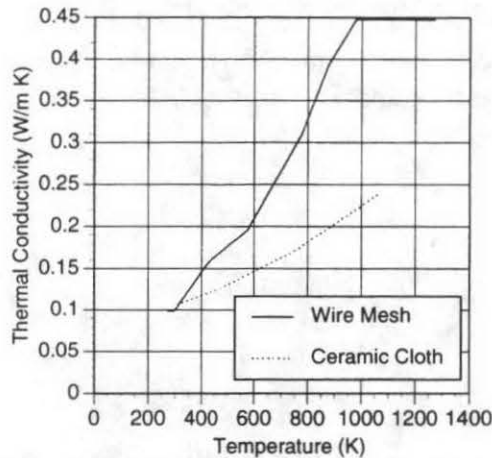


**Figure 3. Thermal Conductivity Of Overpack Layers**

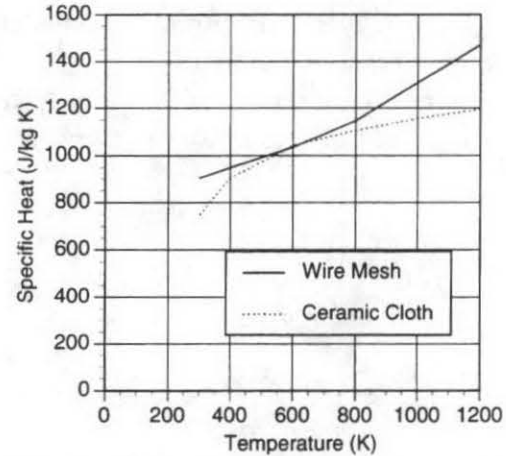


**Figure 4. Specific Heat Of Overpack Layers**

Initially, accuracy was ensured in the COYOTE II model by requiring at least four elements through an overpack layer thickness (design variable). Steep thermal gradients through a layer require multi-element thickness to accurately track temperature changes. If the particular layer was driven toward its lower bound of 2.5 mm, the resulting element size for the entire model became quite small and the model sizes became very large (exceeding 80,000 elements in some cases). In order to reduce excessive CPU time usage, a minimum element size of 1.25 mm was enforced, which reduced the total model size to approximately 19,000 elements when one or more design variables was driven to its lower bound. In this case the thin layer may have as few as 2 or 3 elements through its thickness, balancing accuracy with computational time requirements. Model accuracy was verified by observing that peak temperature differences with the reduced model differed by only 0.03%.

It was assumed that the peak seal area temperature would be most sensitive to variation in design variable  $x_3$  (outer radial thermal layer) due to its proximity to the extreme external heat flux and its large surface area for heat transfer. Constraint surface nonsmoothness with respect to all six design variables was investigated before proceeding with the thermal optimization problem. Initially, severe nonsmoothness was observed with small variation in  $x_3$ , as shown in the stair-stepped data of Figure 5. Some of the discontinuities correlate to changes in the mesh, i.e., changes in the number of elements through the  $x_3$  thickness. Decreasing the time step, as shown in the figure, aided in resolution of large temperature gradients between time steps. And finally, tightening default parameters in COYOTE II, which control iterative matrix solver preconditioners and increase integration accuracy through adaptive time stepping, yielded the relatively smooth, final model data in Figure 5.

## THERMAL OPTIMIZATION RESULTS

A number of thermal design optimization problems were run from different initial feasible designs. Results are presented in Table 1, each using tightened integration and iterative solver controls. Agreement between optimal results for  $x_1$ ,  $x_2$ , and  $x_3$  was good, but limited constraint and objective function sensitivity to design variables  $x_4$ ,  $x_5$ , and  $x_6$  hindered

convergence to unique values of these axial material thicknesses. The radial wire mesh layer,  $x_2$ , is driven to its minimum bound (near zero thickness) in each case and the total thickness of ceramic cloth ( $x_1$  and  $x_3$ ) totalled approximately 7 cm. Cases 1 and 2 used a gradient calculation finite difference step size of 1 percent and Case 3 used 0.1 percent, requiring additional iterations to arrive at a slightly more optimal result.

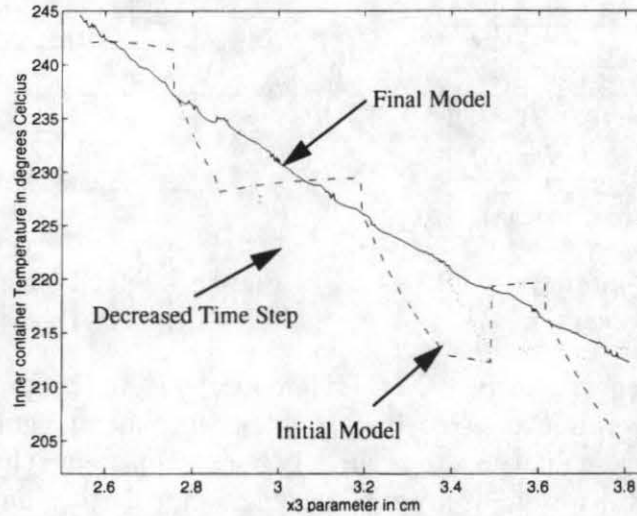


**Figure 5. Improved Constraint Smoothness In Thermal Model. Fine  $X_3$**

**Table 1: Summary Of Thermal Optimization Results**

Case No.	Initial X	Initial Over-Pack Mass	Final X*	Final Over-Pack Mass	$g_{final}$
	$(x_1, x_2, x_3, x_4, x_5, x_6)$		$(x_1, x_2, x_3, x_4, x_5, x_6)$		
1	5.1, 5.1, 5.1, 2.5, 2.5, 2.5 cm	69.6 kg	4.15, 0.25, 2.8, 2.82, 2.65, 1.85 cm	28.3 kg	+0.00289 (232.7° C)
2	3.8, 3.8, 3.8, 1.3, 1.3, 1.3 cm	40.4 kg	4.33, 0.25, 2.67, 2.08, 1.96, 2.92 cm	28.3 kg	+0.00296 (232.7° C)
3	5.1, 5.1, 5.1, 2.5, 2.5, 2.5 cm	69.6 kg	4.28, 0.25, 2.64, 2.91, 2.04, 2.34 cm	28.2 kg	+0.00248 (232.6° C)

A better understanding of the thermal optimization results can be gained from the constraint and objective function sensitivities. Both the peak seal area temperature and the overpack mass are most sensitive (larger gradient or slope) to the outer radial ceramic cloth layer ( $x_3$ ), followed by  $x_1$ ,  $x_2$ ,  $x_6$ ,  $x_4$ , and  $x_5$ . These objective function sensitivity results are due to the ceramic cloth's greater density, and the relative volumes of material added during increases in each layer thickness. The higher sensitivity of the constraint to ceramic cloth layer thicknesses than to wire mesh layer thicknesses is due to the material's thermal diffusivity,  $\alpha$ , which governs transient conduction heat transfer. Thermal diffusivity is defined:

$$\alpha = k/\rho C_p \quad (4)$$

A large value of  $\alpha$  (large  $k$  and/or low  $\rho C_p$ ) implies that a medium is more effective in transferring energy by conduction than it is in storing energy. Units for  $\alpha$  are meters<sup>2</sup>/sec. Factoring in the density differential, the ceramic cloth's lower thermal diffusivity defines the constraint's higher sensitivity to this insulating layer thickness.

The relative lack of sensitivity to design variables  $x_4$ ,  $x_5$ , and  $x_6$  is due to the fact that the circular ends of the overpack present a much smaller area to the external heat flux boundary condition and thus transfer less total heat than material oriented radially ( $x_1$ ,  $x_2$ , and  $x_3$ ). This lack of thermal constraint sensitivity to  $x_4$ ,  $x_5$ , and  $x_6$  is not a concern, since the end-on crush constraint will clearly drive these design variables in the combined thermally and structurally optimized design.

## COMBINED OPTIMIZATION RESULTS

Numerical design optimization of the overpack shape based purely upon thermal design constraints yielded a final overpack mass of 28.3 kg, resulting in a mass savings of 59% from the original design (see Tables 1 and 2 and Figure 6). Similarly, design optimization based upon the end-on crush constraints defined previously, yielded a longer and thinner overpack with a mass of 18.3 kg, 73% lighter than the original design. The end-on dynamic crush constraint tends to drive design variables  $x_4$ ,  $x_5$ , and  $x_6$ , and the peak seal area temperature drives  $x_1$ ,  $x_2$ , and  $x_3$ . Due to slight sensitivity of the end-on constraint to design variables  $x_1$ ,  $x_2$ , and  $x_3$ , the combined optimization problem should yield a unique and more optimum result than merely collecting design variables  $x_1$  through  $x_6$  from separate thermal and structural optimizations.

Performing the combined (structural and thermal constraints) design optimization is a much more difficult undertaking due to the increased number of numerical sensitivities which must be calculated while performing sequential meshing and analysis operations. Six separate combined optimization runs were performed, each from a unique starting design. Unfortunately, consistent navigation to a unique global optimum was not observed. There are two potential causes of this: (1) the existence of true multiple minima in the design space, and (2) the presence of small-scale nonsmoothness in the vicinity of the optimum. Neither of these possibilities has been verified due to limited resources, although the second cause is believed to be true based on the numerical instabilities that have been observed when overpack layer thicknesses (design variables) approach their lower bounds. The minimum mass resultant design of  $\mathbf{X}=(5.6, 2.3, 0.25, 1.6, 26.1, 0.27 \text{ cm})$  has a mass of 42.6 kg, a 38% mass savings over the original design with dimensions of  $\mathbf{X}=(0, 15, 0, 0, 23, 0 \text{ cm})$  (see Table 2). The combined optimum solution is active ( $g_i \cong 0$ ) on the thermal and end-on constraints, and inactive on the side-on constraint.

**Table 2: Combined Structural And Thermal Optimal Results**

	Overpack Mass	$\Delta$ Mass	Optimum $X^*$	Shape
Thermal	28.3 kg	59 %	4.3, 0.25, 2.6, 2.9, 2.0, 2.3 cm	Short & Fat
End-On	18.3 kg	73 %	1.2, 1.8, 0.27, 2.9, 26.7, 2.9 cm	Long & Thin
Combined	42.6 kg	38 %	5.6, 2.3, 0.25, 1.6, 26.1, 0.27 cm	Compromise

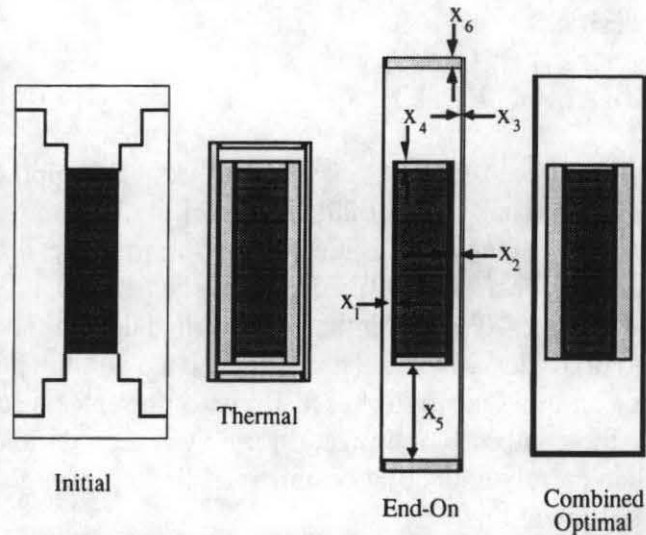


**Figure 6. Optimal Overpack Designs Based On Separate Structural And Thermal, As Well As Combined Optimization Results**

## CONCLUSIONS

The integration of an automatic meshing algorithm, dynamic structural and transient thermal finite element analysis codes, and numerical optimization routines has been achieved. Results thus far indicate that this new package design tool efficiently performs automated, iterative calculations, yielding significant weight savings in an example overpack design problem. Improved overall package safety and efficiency with cost savings in the design and fabrication are hoped to be realized in the near future.

Nonsmoothness of constraint surfaces has been a recurring problem when integrating gradient-based optimization techniques with transient dynamic simulation codes. This ultimately must be addressed with a combined approach of reducing nonsmoothness in analyses and utilizing robust optimization algorithms. Development of simplified yet accurate analysis models is critical in the package design optimization problem due to the high computational cost of iteratively performing numerous analyses. This is a nontrivial undertaking, especially with respect to dynamic crush or impact constraints, due to the highly nonlinear and somewhat discontinuous numerical nature of contact surfaces and high-amplitude stress wave propagation within the container.

As radioactive wastes increase at temporary storage sites and budgets continue to tighten, cost-effective and safe package designs become increasingly paramount. Efforts are continuing to efficiently apply shape optimization to RAM package design. As computational speed rapidly increases along with the need for numerous transport/storage/disposal packages, the numerical design optimization techniques presented here can significantly aid the design process.

## REFERENCES

- Blacker, T. D., *FASTQ User's Manual*, Version 2.1, SAND88-1326, Sandia National Laboratories, Albuquerque, NM (1988).
- Eldred, M. S., Outka, D. E., Fulcher, C. W., and Bohnhoff, W. J., *Optimization of Complex Mechanics Simulations With Object-Oriented Software Design*, Proceedings of the 36th AIAA/ASME/ASCE/AHS/ASC Structures, Structural Dynamics, and Materials Conference, AIAA-95-1433-CP, New Orleans, LA (1995).
- Gartling, D. K., *COYOTE II - A Finite Element Computer Program for Nonlinear Heat Conduction Problems, Part II - Users Manual*, SAND94-1179, Sandia National Laboratories, Albuquerque, NM (1993).
- Harding, D. C., and Eldred, M. S., *Radioactive Material Transportation Package Design Using Numerical Optimization Techniques*, SAND95-0834C, ASME Pressure Vessel and Piping Conference Proceedings on Transport and Storage of Radioactive Materials, PVP-Vol. 307, Honolulu, HI (1995).
- Pierce, J. D., McClure, J. D., Hohnstreiter, G. F., and Gollhofer, K. G., *Type B Plutonium Transport Package Development That Uses Metallic Filaments and Composite Materials*, proceedings of the 10th International Conference on the Packaging and Transportation of Radioactive Materials (PATRAM '92), Yokohama, Japan (1992).
- Taylor, L. M., and Flanagan, D. P., *PRONTO 2D: A Two-Dimensional Transient Solid Dynamics Program*, SAND86-0594, Sandia National Laboratories, Albuquerque, NM (1987).
- Vanderplaats, G. N., *DOT User's Manual - Version 4.10*, VMA Engineering, Colorado Springs, CO (1994).
- Wix, S. D., and Pierce, J. D., *Thermal Characterization of an Advanced Wire Mesh Packaging Material*, Proceedings of the 11th International Conference on the Packaging and Transportation of Radioactive Materials (PATRAM '95), Las Vegas, NV (1995).

## ACKNOWLEDGMENTS

The authors would like to thank M. K. Neilsen, T. Hinnerichs, R. E. Hogan, and S. D. Wix for their contributions, including developing FEA models and performing analyses. The Department of Energy Office of Environmental Restoration and Waste Management Transportation Management Division provided funding for this work.